Backscattering of Laser Radiation on Ultrarelativistic Electrons in a Transverse Magnetic Field: Evidence of MeV-Scale Photon Interference

E. V. Abakumova, M. N. Achasov, D. E. Berkaev, V. V. Kaminsky, N. Yu. Muchnoi,*
E. A. Perevedentsev, E. E. Pyata, and Yu. M. Shatunov

Budker Institute of Nuclear Physics Siberian Branch of the Russian Academy of Sciences and Novosibirsk State University, 630090 Novosibirsk, Russia

(Received 3 November 2012; published 2 April 2013)

In this Letter we report an observation of interference effects in Compton scattering in the experiment held on the VEPP-2000 collider. Infrared laser radiation was scattered head-on the 990 MeV electrons inside the dipole magnet, where an electron orbit radius is about 140 cm. It was observed that the energy spectrum of backscattered photons, measured by a HPGe detector, differs from that defined by the Klein-Nishina cross section and scattering kinematics of free electrons. The explanation of the effect, proposed in terms of classical electrodynamics, is in agreement with QED calculations.

DOI: 10.1103/PhysRevLett.110.140402 PACS numbers: 12.20.Fv, 11.80.−m, 34.80.Pa

Compton scattering is a fundamental process and its properties under usual scattering conditions are well understood within the Dirac QED theory and described by the Klein-Nishina formula [1]. Inverse Compton scattering (ICS) of laser radiation on the ultrarelativistic electrons is widely used for production of intense beams of high-energy and low-bandwidth polarized photons [2–7], for measurement of the electron beam polarization [8–10], energy [11–13], size [14,15], etc. With increase of laser power density, the Klein-Nishina cross section is known to be modified by nonlinear (multiphoton) Compton scattering [16–18].

Current research focuses on one extension of linear ICS. In our case, the scattering of a laser photon on the ultrarelativistic electron occurs when the electron trajectory is not straight.

VEPP-2000 [19] is an e^+e^- collider, operating in the energy range $0.2 \leq E_{\text{c.m.}} \leq 2.0$ GeV. It has eight equal dipole magnets with electron bend radius $R = 140$ cm. The monochromatic cw laser radiation ($\lambda_0 = 10.591\ \mu$m) is injected into the collider vacuum chamber towards the electron beam according to Fig. 1. The laser and electron beam interaction occurs inside the 3M1 magnet and backscattered photons hit the HPGe detector, located in the orbit plane $\simeq 225$ cm away from the interaction area.

According to kinematics of ICS, the maximum energy of backscattered photons $\hbar\omega_{\max} \simeq 4\gamma^2\hbar\omega_0$ for a head-on collision, where $\gamma = E/m$ is the electron Lorentz factor. In the absence of the constant electromagnetic (EM) field, the energy spectrum of Compton photons has an abrupt edge at this energy, which is often used as a reference energy point for calibration purposes [11–13]. The measured energy spectrum of laser backscattered photons is shown in Fig. 2.

Energy scale calibration for this measurement is based on 583.191, 860.564, and 2614.511 keV lines of ^{208}Tl β^- decay. The amplitude oscillations in the spectrum are clearly seen at least in the range from 1600 to 1800 keV, while kinematics gives $\hbar\omega_{\max} \simeq 1755$ keV. At lower energies these oscillations are smeared by Compton scattering in the HPGe detector. One can see some homogeneous background and notice the presence of surrounding radiation, like a 1460 keV peak from ^{40}K electron capture decay γ-rays.

In order to understand our observations, let us consider the interaction between an electron and a laser wave in terms of classical electrodynamics.

A laser beam propagates along a tangent towards the electron beam orbit; see Fig. 1. It is focused by two ZnSe lenses providing the transverse waist size of about 1 mm. Thus, the approximate length of the interaction region is about $L_{\text{int}} \simeq 10$ cm, which corresponds to an electron bending angle $\theta_{\text{int}} = L_{\text{int}}/R \simeq 70$ mrad (Fig. 3). Practically, the overlap of laser and electron beams is achieved by means of the positive feedback system, which finds the maximum rate of backscattered photons, counted by the HPGe detector, via fine-tuning of transverse and longitudinal positions of the laser beam waist.

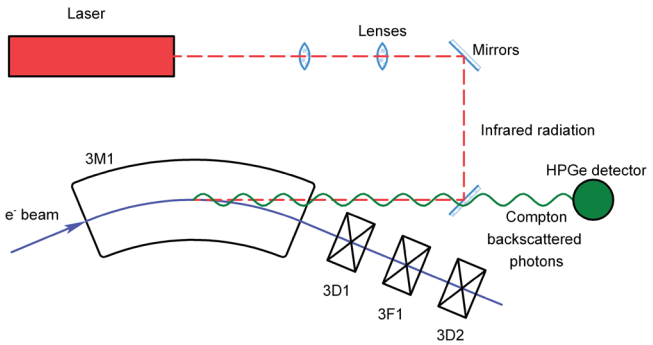

FIG. 1 (color online). Experimental layout. CO_2 laser: Coherent GEM Select 50. HPGe detector: Ortec GMX25-70-A.

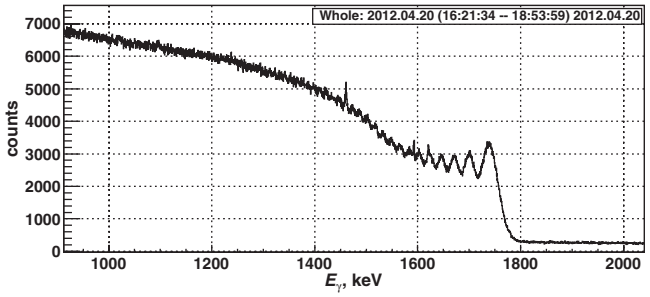

FIG. 2. The measured energy spectrum of backscattered photons. $E \simeq 990$ MeV, $\hbar\omega_0 = 0.117$ eV, acquisition time 2.5 h.

A typical radiation angle of an ultrarelativistic electron $\theta_{\rm rad} \simeq 1/\gamma$, which is about 0.5 mrad at $E \simeq 1$ GeV. Thereby, $\theta_{\rm rad}$ is 2 orders of magnitude smaller than $\theta_{\rm int}$. This case is in general quite similar to the case of, e.g., synchrotron radiation in a uniform field: whatever the radiation properties, they are the same for any direction, lying in the plane orthogonal to the electron orbit plane and tangent to the electron orbit. In other words, it is enough to find the properties of backscattered laser radiation, propagating in the planes orthogonal to the plane of Fig. 3 and with $\phi = 0$ (see Fig. 3).

Assuming possible interference of the waves, emitted from points A and C in a certain direction, it is necessary to determine the phase difference between these two waves. In our case the direction of radiation is specified by two angles: $\phi \equiv 0$ and ψ, the vertical angle with respect to the orbit plane. The time of an electron flight from point A to point C is

$$t_e = \frac{2R\theta}{v} = \frac{2R\theta}{\beta c}. \tag{1}$$

The wave front of the radiation, emitted from point A at a vertical angle ψ, will spatially coincide with the wave front, emitted from point C at the same angle after

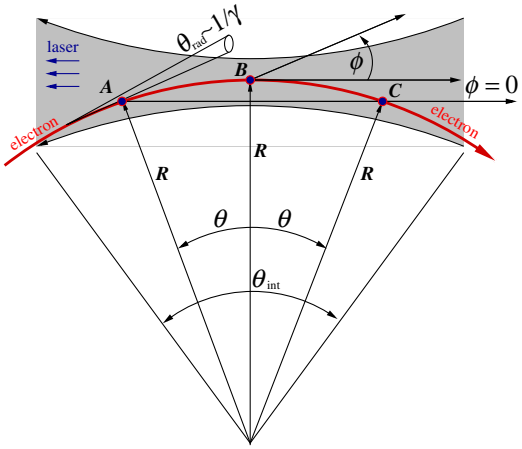

FIG. 3 (color online). Sketch of the laser-electron interaction area. $R = 140$ cm is the electron orbit radius.

$$t_\gamma = \frac{2R\sin\theta}{c}\cos\psi. \tag{2}$$

The phase difference between these waves for a certain wavelength λ is determined by the laser radiation wavelength λ_0:

$$\Delta\Phi = 2\pi c\left(\frac{t_e}{\lambda} - \frac{2t_e}{\lambda_0} - \frac{t_\gamma}{\lambda}\right) = \frac{2R}{c}\left(\frac{\theta}{\beta}(\omega - 2\omega_0) - \omega\sin\theta\cos\psi\right), \tag{3}$$

where we take into account the laser wave phase shift while the electron propagates from A to C. Since $\theta, \psi, 1/\gamma \ll 1$, Eq. (3) transforms to

$$\Delta\Phi \simeq \frac{\omega R}{c}\left[\theta\left(\frac{1}{\gamma^2} - \frac{4\omega_0}{\omega} + \psi^2\right) + \frac{\theta^3}{3}\right]. \tag{4}$$

When $\Delta\Phi$ is an odd (even) multiple of π one observes an interference minimum (maximum) of the scattered wave. The scattered field amplitude is evaluated by integration along the electron path:

$$U \propto \omega\int_0^\infty (e^{i(\Delta\Phi/2)} + e^{-i(\Delta\Phi/2)})d\theta = 2\omega\int_0^\infty \cos\frac{\Delta\Phi}{2}d\theta. \tag{5}$$

Change of the integration variable $\theta \to \xi = \theta(\omega R/2c)^{1/3}$ allows one to rewrite the expression (5) as

$$U \propto \omega^{2/3}\,{\rm Ai}(x), \tag{6}$$

where

$$x = \left(\frac{\omega R}{2c}\right)^{2/3}\left(\frac{1}{\gamma^2} - \frac{4\omega_0}{\omega} + \psi^2\right), \tag{7}$$

and ${\rm Ai}(x) = \frac{1}{\pi}\int_0^\infty \cos(xt + \frac{t^3}{3})dt$ is the Airy function. The intensity of a scattered wave is

$$I = |U|^2 \propto \omega^{4/3}\,{\rm Ai}^2(x). \tag{8}$$

Expression (8) is the solution for the angular distribution of the backscattered radiation spectral power density. According to the above approach, the result does not depend on the type of particle the laser wave is scattered on. A similar solution can be obtained by the analysis of the Fourier harmonics of the radiation field of a charged particle [20].

The HPGe detector active volume has cylindrical shape of about 7 cm height and 5 cm diameter, so it covers the vertical scattering angle $\psi < \psi_D \simeq 15$ mrad, and since $\psi_D \gg 1/\gamma$, one can consider it as $\psi_D = \infty$. To obtain the energy spectrum of scattered photons, one should integrate expression (8) over the vertical angle ψ and divide the result by the photon energy $\hbar\omega$:

$$\frac{d\dot{N}_\gamma}{d\hbar\omega} \propto \omega^{1/3} \int_0^\infty \mathrm{Ai}^2(x) d\psi. \quad (9)$$

The integral in Eq. (9) can be expressed via the primitive of the Airy function using the relation

$$\int_0^\infty \mathrm{Ai}^2(a+by^2)dy = \frac{1}{4\sqrt{b}} \int_z^\infty \mathrm{Ai}(z')dz', \quad z = 2^{2/3}a. \quad (10)$$

Hence, the final form of the interference factor is

$$\frac{d\dot{N}_\gamma}{d\hbar\omega} \propto \int_z^\infty \mathrm{Ai}(z')dz' = \frac{1}{3} - \int_0^z \mathrm{Ai}(z')dz', \quad (11)$$

where

$$z = \left(\frac{\omega R}{c}\right)^{2/3} \left(\frac{1}{\gamma^2} - \frac{4\omega_0}{\omega}\right). \quad (12)$$

The results, represented by Eqs. (8) and (11), are shown in Fig. 4. The distribution of scattered wave intensity as a function of the photon energy and its scattering angle ψ shows the sought-for interference effect with 100% intensity modulation. The interference is still evident in the energy spectrum of scattered photons.

Let us point out that, in the presence of constant EM field in the scattering area, the abrupt high-energy edge in the energy spectrum of backscattered photons no longer exists; see Fig. 4. The spectrum shape, similar to Eq. (11), was obtained in semiclassical theory of electromagnetic processes [21].

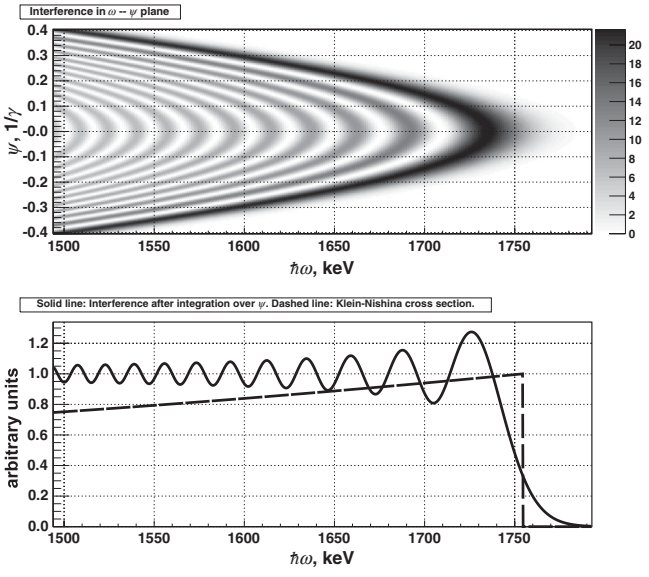

FIG. 4. Upper plot: Interference of scattered waves according to Eq. (8) in ω-ψ plane. Lower plot: Solid line, the energy distribution of backscattered photons according to Eq. (11); dashed line, the same according to Klein-Nishina cross section with the abrupt edge given by the ICS kinematics. $E = 990$ MeV, $\hbar\omega_0 = 0.117$ eV, $R = 140$ cm.

Until now we have not yet taken into account the quantum recoil. To do this one should, according to Ref. [22], substitute $\omega \to \omega E/(E - \hbar\omega)$ in Eq. (12).

An electron radius is coupled with its energy and magnetic field strength by the balance between the Lorenz and centrifugal forces: $\beta E = cBR$. It is convenient to perform $R \to E/(cB)$ substitution in Eq. (12).

After these substitutions are made, let us introduce new variables [23]:

$$u = \frac{\hbar\omega}{E - \hbar\omega}, \qquad \kappa = \frac{4E\hbar\omega_0}{m^2}, \qquad \chi = \frac{E}{m}\frac{B}{B_0}, \quad (13)$$

where $B_0 = m^2/\hbar c^2 = 4.414 \times 10^9$ T is the Schwinger field strength. Now Eq. (12) looks like

$$z = (u/\chi)^{2/3}(1 - \kappa/u). \quad (14)$$

The influence of constant EM field on the cross section of Compton scattering was studied in Ref. [23], where the energy spectrum of scattered photons was obtained from the solution of the Dirac equation. The result is

$$\frac{d\dot{N}_\gamma}{d\hbar\omega} \propto \nu_1 \int_z^\infty \mathrm{Ai}(z')dz' + \nu_2\,\mathrm{Ai}'(z) + \nu_3\,\mathrm{Ai}(z), \quad (15)$$

where

$$\nu_1 = \frac{1}{8}\left\{2 + \frac{u^2}{1+u} - 4\frac{u}{\kappa} + 4\left[\frac{u}{\kappa}\right]^2 - 16\left[\frac{u}{\kappa}\right]^2\left[\frac{\chi}{\kappa}\right]^2\right\},$$
$$\nu_2 = -\left[\frac{u}{\kappa}\right]^{4/3}\left[\frac{\chi}{\kappa}\right]^{2/3}\left\{4\left[\frac{\chi}{\kappa}\right]^2 + \frac{u^2}{2(1+u)}\left[1 + 4\left[\frac{\chi}{\kappa}\right]^2\right]\right\},$$
$$\nu_3 = \left[\frac{u}{\kappa}\right]^{2/3}\left[\frac{\chi}{\kappa}\right]^{4/3}\left\{3 - 2\frac{u}{\kappa} + \frac{u^2}{2(1+u)}\left[3 - 4\frac{u}{\kappa}\right]\right\}. \quad (16)$$

In the case relevant to our experiment, $u \lesssim 10^{-3}$, $\kappa \lesssim 2 \times 10^{-3}$, and $\chi \lesssim 10^{-6}$. The influence of constant field on the process of Compton scattering depends on the χ/κ ratio. Since $u/\kappa \simeq 0.5$ and $\chi/\kappa \lesssim 0.5 \times 10^{-3}$, the last term in ν_1 in Eq. (16) may by omitted, and ν_1 becomes just the Klein-Nishina cross section. The values of ν_2 and ν_3 in Eq. (16) are significantly smaller than ν_1 for the same reason. In this case one can see that the QED result is the product of Eq. (11) by the Klein-Nishina cross section.

In order to compare the measured energy spectrum with the theory predictions, it is necessary to take into account the energy spread of the electrons in the beam. Let δ be the relative energy shift of an electron energy E' from the average energy E of electrons in the beam: $E' = E(1+\delta)$. The appropriate weight function for the electron energy distribution will be

$$w(\delta) = \frac{1}{\sqrt{2\pi}\sigma} \exp\left(-\frac{\delta^2}{2\sigma^2}\right), \quad (17)$$

where by definition σ is the relative beam energy spread. In the case $\sigma \ll 1$, the linear approximation for the coupling between z and δ will be adequate. From Eq. (14)

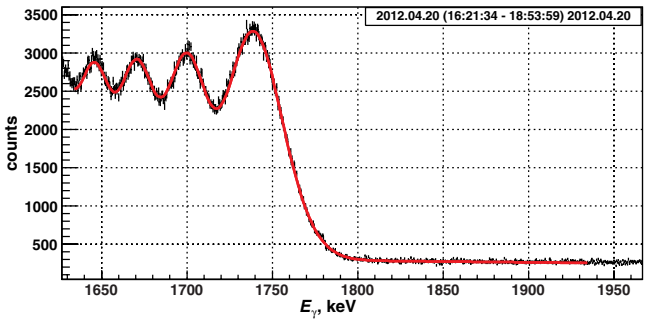

FIG. 5 (color online). The edge of the energy spectrum with the fit result: $\chi^2/\text{d.o.f} = 773.0/745$, $E = 993.662 \pm 0.016$ MeV, $B = 2.3880 \pm 0.0044$ T, $\sigma = 810 \pm 40$ ppm.

$$z(\delta) \simeq z - \eta \times \frac{\delta}{\sigma}, \qquad \eta \simeq \sigma \times \frac{4}{3}\left(1 + \frac{1}{2}\frac{\kappa}{u}\right)\left(\frac{u}{\chi}\right)^{2/3}. \quad (18)$$

The energy spectrum transformation due to nonzero energy spread in the electron beam is established by convolution of Eqs. (11) and (17), yielding the final result:

$$\frac{d\dot{N}_\gamma}{d\hbar\omega} \propto \mathcal{F}(\omega, E, B, \sigma) = e^{-\eta^6/24} \int_{z+\eta^4/4}^{\infty} e^{z'\eta^2/2}\,\mathrm{Ai}(z')dz'. \quad (19)$$

Let us introduce a combined function to describe the shape of the experimental spectrum:

$$f(\omega) = \mathcal{A}\,\mathcal{F}(\omega, E, B, \sigma) + \mathcal{B}(\omega), \quad (20)$$

where $\mathcal{B}(\omega) = p_0 + p_1(\omega - \omega_{\max})$ is the estimation of the background shape. $f(\omega)$ has six free parameters: $\mathcal{A}$ is the normalization parameter, E is the average energy of electrons in the beam, B is the magnetic field in the interaction area, σ is the relative electron energy spread, p_0 and p_1 describe the linear background, while the laser photon energy $\hbar\omega_0 = 0.117065223$ eV. The edge of the experimental spectrum is well fitted with $f(\omega)$; see Fig. 5. The fitting results indicate that the properties of the observed phenomenon provide an opportunity for a simultaneous measurement of average electron energy, $\Delta E/E \simeq 2 \times 10^{-5}$, EM field in the scattering area, $\Delta B/B \simeq 0.2\%$, and beam energy spread, $\Delta\sigma/\sigma \simeq 4\%$.

In order to implement this, further careful studies of the spectrum shape are required. The experimental results are consistent with either QED or classical theory predictions: the observed phenomenon can be explained as the interference of photons with $\lambda \sim 10^{-10}$ cm. The peculiar scattering geometry looks promising as a new diagnostic tool for accelerator-based experiments.

The authors are grateful to V. E. Blinov, A. G. Kharlamov, A. A. Korol, A. A. Krasnov, S. I. Serednyakov, Yu. A. Tikhonov, and V. M. Tsukanov for support of this work and to S. I. Eidelman, A. I. Milstein, Z. K. Silagadze, and V. M. Strakhovenko for useful discussions. The work is supported by the Ministry of Education and Science of the Russian Federation, by RF Presidential Grant for Scientific Schools NSh-6943.2010.2, and by RFBR Grants No. 12-02-01250-a, No. 12-02-00065-a, and No. 11-02-00276-a.

*N.Yu.Muchnoi@inp.nsk.su

[1] O. Klein and T. Nishina, Z. Phys. **52**, 853 (1929).
[2] J. Ballam, G. Chadwick, R. Gearhart, Z. G. Guiragossian, P. Klein *et al.*, Phys. Rev. Lett. **23**, 498 (1969).
[3] M. Preger, B. Spataro, R. Bernabei, M. de Pascale, and C. Schaerf, Nucl. Instrum. Methods, Sect. A **249**, 299 (1986).
[4] S. Akhmadaliev, G. Kezerashvili, S. Klimenko, R. Lee, V. Malyshev *et al.*, Phys. Rev. Lett. **89**, 061802 (2002).
[5] V. Litvinenko, B. Burnham, M. Emamian, N. Hower, J. Madey *et al.*, Phys. Rev. Lett. **78**, 4569 (1997).
[6] K. Kawase, Y. Arimoto, M. Fujiwara, S. Okajima, M. Shoji, S. Suzuki, K. Tamura, T. Yorita, and H. Ohkuma, Nucl. Instrum. Methods Phys. Res., Sect. A **592**, 154 (2008).
[7] S. Amano, K. Horikawa, K. Ishihara, S. Miyamoto, T. Hayakawa, T. Shizuma, and T. Mochizuki, Nucl. Instrum. Methods Phys. Res., Sect. A **602**, 337 (2009).
[8] M. Beckmann, A. Borissov, S. Brauksiepe, F. Burkart, H. Fischer *et al.*, Nucl. Instrum. Methods Phys. Res., Sect. A **479**, 334 (2002).
[9] M. Baylac, E. Burtin, C. Cavata, S. Escoffier, B. Frois *et al.*, Phys. Lett. B **539**, 8 (2002).
[10] M. Fukuda, T. Aoki, K. Dobashi, T. Hirose, T. Iimura *et al.*, Phys. Rev. Lett. **91**, 164801 (2003).
[11] R. Klein, T. Mayer, P. Kuske, R. Thornagel, and G. Ulm, Nucl. Instrum. Methods Phys. Res., Sect. A **384**, 293 (1997).
[12] V. E. Blinov, A. V. Bogomyagkov, N. Yu. Muchnoi, S. A. Nikitin, I. B. Nikolaev, A. G. Shamov, and V. N. Zhilich, Nucl. Instrum. Methods Phys. Res., Sect. A **598**, 23 (2009).
[13] E. Abakumova, M. Achasov, V. Blinov, X. Cai, H. Dong *et al.*, Nucl. Instrum. Methods Phys. Res., Sect. A **659**, 21 (2011).
[14] Y. Honda, N. Sasao, S. Araki, Y. Higashi, T. Okugi *et al.*, Nucl. Instrum. Methods Phys. Res., Sect. A **538**, 100 (2005).
[15] A. Aryshev, G. Blair, S. Boogert, G. Boorman, A. Bosco *et al.*, Nucl. Instrum. Methods Phys. Res., Sect. A **623**, 564 (2010).
[16] F. V. Hartemann and A. K. Kerman, Phys. Rev. Lett. **76**, 624 (1996).
[17] C. Bula *et al.* (E144 Collaboration), Phys. Rev. Lett. **76**, 3116 (1996).
[18] M. V. Galynskii, E. Kuraev, M. Levchuk, and V. I. Telnov, Nucl. Instrum. Methods Phys. Res., Sect. A **472**, 267 (2001).
[19] D. Berkaev, D. Shwartz, P. Shatunov, Y. Rogovskii, A. Romanov *et al.*, JETP **113**, 213 (2011).

[20] L. D. Landau and E. M. Lifshits, *The Classical Theory of Fields*, Course of Theoretical Physics Vol. 2 (Butterworth-Heinemann, Burlington, 1975), pp. 176–187.

[21] V. N. Baier, V. M. Katkov, and V. M. Strakhovenko, JETP **73**, 945 (1991).

[22] V. N. Baier, V. M. Katkov, and V. S. Fadin, *Radiation by Relativistic Electrons* (Atomizdat, Moscow, 1973).

[23] V. C. Zhukovsky and I. Herrmann, J. Nucl. Phys. **14**, 150 (1971).